JOURNAL OF APPLIED ELECTROCHEMISTRY 6 (1976) 301–310

Electrodeposited manganese dioxide with preferred crystal growth

E. PREISLER

Hoechst AG, Werk Knapsack, Anorganische Forschung, D 5030 Hürth, near Cologne

Received 2 June 1975

Manganese dioxide, prepared by the anodic oxidation of hot sulphuric acid-containing manganese sulphate solutions, is a polycrystalline material with a random distribution of the lattice orientations of the micro crystals. Electrodeposited manganese dioxide precipitating under similar conditions from acidic solutions of manganese chloride, nitrate, or perchlorate exhibit clearly a fibrous structure, the axes of the single fibres being parallel with the direction of growth. X-ray diffraction shows a marked texture of growth. All the fibrous forms of manganese dioxide that have been described are of the γ-variety. They can easily be cleft in planes parallel to the direction of their growth.

Even the manganese dioxide crystallizing from sulphate solutions often has a growth texture which, though less marked, is still detectable by X-ray analysis. Sometimes the crystal orientation is so pronounced that this material can also be cleft.

In the hot spent electrolyte of the technical process, manganese dioxide of the γ-variety is deposited on non-polarized surfaces, possibly by a very slow hydrolysis of manganese(III)ions. This manganese dioxide has a bulk density of $4{\cdot}5\ \mathrm{g\,cm^{-3}}$ and its crystals, too, are oriented with regard to the direction of their growth.

1. Introduction

Manganese dioxide is manufactured on an industrial scale by the anodic oxidation of hot sulphuric acid-containing manganous sulphate solutions. The ground material is mainly used for cathodes in primary batteries. Under the usual technical conditions [1] manganese dioxide is deposited on the anode as a solid having a bulk density of about $3{\cdot}9$–$4{\cdot}0\ \mathrm{g\,cm^{-3}}$. It is polycrystalline and no defined crystal surfaces can be observed. X-ray diffraction patterns indicate the γ-variety, though some of the reflections which have been described in the literature to be due to the γ-variety are not apparent. The reflections are less sharp and much broader than those of natural pyrolusite, indicating a relatively poor state of crystallization. The large active surface of about $40\ \mathrm{m^2\,g^{-1}}$ (BET surface area) is also characteristic of a large number of lattice defects. Koshiba and Nishizawa [2] have shown, however, that the 'electrodeposited manganese dioxide' that is prepared industrially is not always free of texture, and that in spite of the low degree of crystallization there may be an orientation of crystals which can be detected by comparing the intensity of the reflections obtained by taking X-ray diagrams parallel or normal to the sample surface.

In 1966, electrodeposited manganese dioxide having properties essentially different from those that had been known up to then was described by Amano, Kumano, Nishino and Noguchi [3]. This material, described by the authors as fibrous manganese dioxide, is prepared by the anodic oxidation of hot manganese chloride solutions containing hydrochloric acid. It is deposited in solid form on graphite or platinized titanium anodes. The fibrous manganese dioxide thus obtained has an excellent orientation, a higher degree of crystallization and needle shaped crystallites. The direct current resistivity in the direction parallel to the direction of growth is in the range of 8–12 Ω cm and is much lower than the resistivity in the direction normal to the direction of growth which the authors found to be between 275–330 Ω cm. The material can easily be cleft in the direction parallel

Table 1. *List of manganese dioxides under investigation*

Designation	*Bath*	*Additions* ($g l^{-1}$)	*Current density* ($A dm^{-2}$)	*Type of texture**	*Cleavable*	*Bulk density* ($g cm^{-3}$)	*Remarks*	*Literature*
FEMD-C	$MnCl_2/HCl$	–	$\leqslant 5$	II	Yes	4·0	Technically pure electrolyte	[3]
FEMD-N	$Mn(NO_3)_2/HNO_3$	–	$\leqslant 3–4$	II	Yes	4·0	Technically pure electrolyte	[4]
FEMD-P	$Mn(ClO_4)_2/HClO_4$	–	$\leqslant 7–9$	II	Yes	4·0		This work
FEMD-Ac	$Mn(CH_3COO)_2/CH_3COOH$	–	1		Yes	Not determined	Soft material of low density	This work
FEMD-S	$MnSO_4/H_2SO_4$	–	1·2	I	Yes	3·2	Splitting properties less pronounced	This work
EMD-S	$MnSO_4/H_2SO_4$	–	$< 2·5$	I	No	3·9–4·1	Technical product	[1, 2]
EMD-S	$MnSO_4/H_2SO_4$	Fe^{2+} : 3	1	II	No	4·0		This work
EMD-S	$MnSO_4/H_2SO_4$	V^{4+} : 0·1	1	II	No	4·0	EMD content: 0·2% vanadium	This work
EMD	$Mn(SO_3NH_2)_2HSO_3NH_2$	–	1	Not determined	No	Not determined		This work
EMD	$Mn(SiF_6)_2/H_2SiF_6$	–	1	Not determined	No	Not determined		This work
EMD-S	$MnSO_4/H_2SO_4$	–	$< 2·5$	No	No	3·8	Textureless	This work
HMD	$MnSO_4/H_2SO_4$	–	0	I	No	4·5		This work

* For details see Section 7.

to the direction of growth. The orientation of the axis of the fibres coincides with the normal of the 110 plane of ramsdellite. An analogous fibrous manganese dioxide can be produced from nitric acid manganous nitrate baths [4].

Experiments in our laboratory have shown that in the case of acidic manganous sulphate solutions both the textured and untextured deposits occur, depending on not well-known conditions of electrolysis. Moreover, the preparation of fibrous manganese dioxide is not restricted to the use of chloride or nitrate baths but perchloric acid-containing manganous perchlorate solutions yield fibrous electrolytic manganese dioxide too, within a broad current density range of 2–50 mA cm^{-2}. This product has an excellent crystal orientation and very good cleavage properties.

From manganous acetate baths an anodic deposit can be obtained which shows some indication of a fibrous structure, but has a low bulk density and is very soft and brittle.

Furthermore, it has been possible to produce from sulphate baths a manganese dioxide which is fibrous too, and has cleavage properties which differ distinctly from the type described by the Japanese authors with regard to the appearance of the surface of fracture as well as to the intensity shifts of the diffraction lines when changing the direction of the incident beam in the diffractometer.

It has moreover been found that under certain conditions manganese dioxide is deposited in the electrolyte of commercial plants by an obviously non-electrochemical reaction which perhaps is a hydrolysis reaction of manganese(III)ions. This deposit which has a high density is of great hardness but possesses a growth texture which is not fibrous. The results of these examinations will be given in this paper and be compared with the Japanese findings.

2. Designation of the various types of manganese dioxide

All types of manganese dioxide discussed here are crystallized in the form of the γ-variety. The samples obtained in the different ways are denoted in this paper by the following designations:

EMD: all types of manganese dioxide, prepared by anodic oxidation, which have no fibrous structure (electrodeposited manganese dioxide).

FEMD: all types of manganese dioxide prepared by anodic oxidation having a fibrous macrostructure (fibrous EMD).

FEMD-C (-N, -P, -S): fibrous EMD prepared from chloride, nitrate, perchlorate, or sulphate bath, respectively.

HMD: manganese dioxide that has grown by disproportionation and hydrolysis as described above (hydrolytic MD).

3. Experimental

All electrodeposited manganese dioxide samples have been prepared under conditions similar to the technical process for EMD, e.g. temperature 95° C, concentration of manganous salt in the electrolyte 0·7 M, concentration of the corresponding acid 0·7 M; anodes: lead or graphite, current density 1 A dm^{-2}, deposition time: several days. Table 1 gives a summary of the materials studied here and the range of deviation from standard conditons that have been used.

The potential sweep diagrams for a graphite electrode in sulphuric acid or nitric acid-containing manganous salt solutions were obtained using a Jaissle Potentiostat 1000 T-B in conjunction with a Philips Function Generator PM 5168 and a Tektronix storage oscilloscope. The range of the linear potential sweep was from $+0{\cdot}68$ to $+1{\cdot}58$ V versus the normal hydrogen electrode.

The determination of the BET surface has been performed on powder samples of manganese dioxide passing a sieve of 100 mesh (BSS 410). These samples were subjected to a heat treatment at 80° C in vacuo until weight constancy was reached. Then the adsorption isotherms at $-196°$ C of nitrogen were taken at pressures of 65, 130, 200 and 260 mbar with an accuracy of about 1%. The BET-surface values depend to a certain extent on the particle size and are under the given conditions reproducible to about 10% for each type of sample.

4. Electrochemical examination

The electrochemical formation of manganese dioxide proceeds according to the following basic reaction scheme:

$$\begin{aligned} 2Mn^{2+} &\longrightarrow 2Mn^{3+} + 2e \\ 2Mn^{3+} &\longrightarrow Mn^{2+} + Mn^{4+} \\ Mn^{4+} + 2H_2O &\longrightarrow MnO_2 + 4H^+. \end{aligned}$$

According to this rather simplified scheme manganese dioxide is obtained in solid form at current densities of about 1 A dm^{-2} and temperatures of 90–95° C. At these temperatures one generally gets the best current yields, which in moderately acidic solutions (0·5–1 M) typically amount to 90–95%. When as a result of raising the acid concentration the disproportionation of the primarily formed tervalent manganese ions and the hydrolysis of the subsequently forming quadrivalent manganese ions are more and more retarded, the current yield decreases [5]. Owing to their longer lifetime a proportion of the manganese(III)ions diffuse off the pre-anode layer into the bulk solution where the reaction is completed by the formation of colloidal manganese dioxide or, if this reaction proceeds very slowly, solid manganese dioxide, which grows in various forms on the walls of the containers.

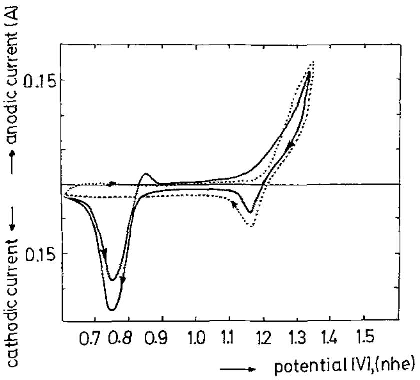

Fig. 1. Potentiodynamic current–voltage curves of a graphite electrode in solutions of 0·5 M $MnSO_4$–0·7 M H_2SO_4 (dotted line) and 0·5 M $Mn(NO_3)_2$–1 M HNO_3 (solid line) at 90° C. Electrode geometrical surface: 4 cm^2. Sweep speed: 15 mV s^{-1}.

In hydrochloric and nitric acid baths, no formation of colloids has been observed. Obviously quadrivalent manganese ions or colloidal manganese dioxide react rapidly with hydrochloric acid. In nitric acid baths the formation of nitrous oxide occurs. At low nitric acid concentration the cell voltage is about 2·0–2·4 at current densities of 1 A dm^{-2}, which is the same value as for sulphate baths. At elevated nitric acid concentrations, the cell voltage drops to values within the range of 0·5–0·8 V. The cyclic current voltage diagram (Fig. 1) shows that in this case the potential of the manganese dioxide electrode has practically the same value as in the sulphate bath, but that at potentials of about 820 mV (nhe), a strong cathodic current peak appears which may be ascribed to the reduction of nitric acid to nitrous acid. So the potential of the cathode is more positive by 1·2–1·3 V because the nitrate/nitrite reaction occurs in preference to the hydrogen evolution reaction. Consequently, the overall cell voltage at a given current density drops by this value.

With a graphite electrode, the active surface will be possibly blocked by reaction products formed during the reduction of nitric acid. If the electrode potential is shifted to values below + 770 mV (nhe), the cathodic current decreases and drops to fairly low values, while it increases again when the potential reaches the hydrogen evolution potential. As the nitric acid/nitrous acid cathodic current peak is reversible with respect to the direction of the potential scan, the behaviour of the graphite electrode is similar to the so-called 'anode effect' which often can be observed at gas-evolving anodes.

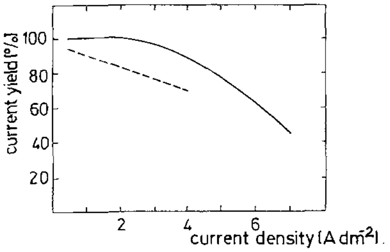

Fig. 2. Dependence of the current yield for the deposition fo FEMD-P and FEMD-N on the anodic current density at 90° C. Solutions: 0·6 M $HClO_4$–0·73 M $Mn(ClO_4)_2$ (solid line) and 0·6 M HNO_3–0·73 M $Mn(NO_3)_2$ (dotted line).

The cathodic current peak at + 1170 mV is caused by the reduction of manganese dioxide that has been deposited while the electrode was polarized more positive than + 1220 mV.

When the electrolysis cell is not provided with a diaphragm, the reoxidation of the free nitrous acid that has been formed leads to decreases in current yield for the electrodeposition of manganese dioxide. Fig. 2 illustrates these losses in terms of the anodic current densities for the nitrate and the perchlorate systems at equal molar concentrations.

FEMD-P precipitates from perchloric acid/manganous perchlorate baths with good current yield at concentrations and current densities within a broad range. At current densities of up to 50 mA cm^{-2}, the precipitate is a markedly fibrous and solid product. At higher current densities a more brittle and soft product is formed which, however, preserves its fibrous structure.

5. Survey on the conditons for the appearance of a growth texture

Although much experimental material concerning the preparation of texturized manganese dioxide has been collected, no explanation for the appearance of the texture nor for the formation of the fibrous structure has yet been suggested. The cause can neither be found in the anion of the electrolyte nor in the presence of certain impurities. Temperature and current densities are not determining parameters either. Nor does any correlation exist between the fibrous nature or cleavage properties and a definite type of texture, as X-ray diagrams have shown. In general it may be said that absolutely textureless solid electrolytic manganese dioxide is a rare exception, and that manganese dioxides that cannot been cleft often exhibit a growth texture. However, in all cases that have hitherto been known, cleavable manganese dioxide has a growth texture, too, which is so marked that the surfaces of precipitates of that kind are always very bright whereas precipitates that cannot be cleft always have mat surfaces. The known materials and the conditions under which they form are summarized in Table 1.

6. Microscopic examinations

The crystal orientation of the commercial electrolytic manganese dioxide is either undetectable or only detectable by X-ray examination of samples having the form of a block. All EMD types have mat surfaces and smooth, non-structured fractures as is shown in Fig. 3. Even at high magnification no grain boundaries or crystallite surfaces can be distinguished (Fig. 8a). EMD has a tendency to form fine cracks when samples extracted from the hot electrolysis bath are cooled down to ambient temperature. Consequently the material is often broken to irregular pieces when being cut by means of a diamond saw.

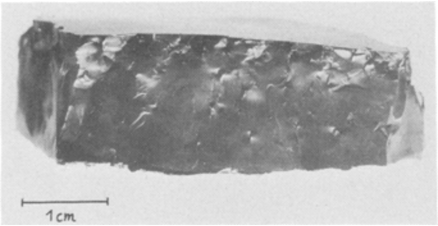

Fig. 3. EMD.

Isotropic EMD, having no growth structure, is in general resistent to fracture and very hard and often has fine pores and a surface structure which indicate the influence of convective flows within the cells.

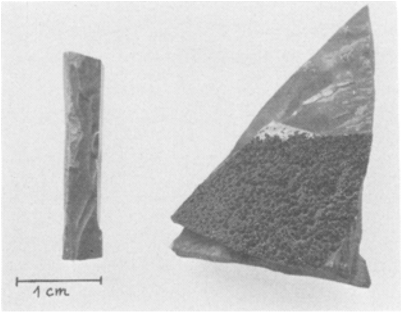

Fig. 4. HMD.

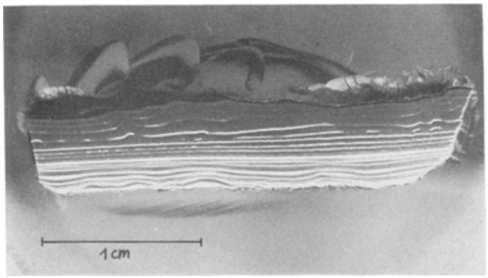

Fig. 5. HMD. Section parallel to the direction of growth.

HMD is a very solid, hard, and flawless manganese dioxide (Figs. 4 and 5). The polished cross-sectional surface of this material presents many wavy strips which are approximately parallel to the surface of the deposit. They are due to changes in the conditions of deposition which lead to changes in the light-reflection properties of the manganese dioxide.

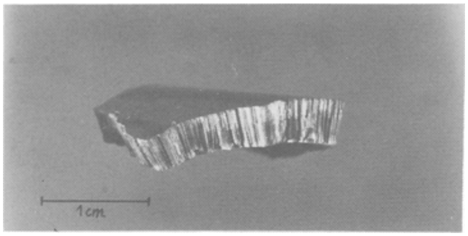

Fig. 6. FEMD-N.

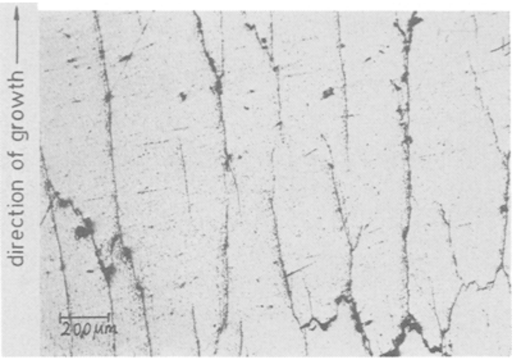

Fig. 7. FEMD-N. Section parallel to the direction of growth (polished and etched with dilute H_2O_2–H_2SO_4-solution).

The microscopic structure of fibrous manganese dioxide has been described by Nishino [6]. As far as it is recognizable his findings regarding FEMD-C and FEMD-N are identical with the results we obtained with FEMD-N and FEMD-P. Fig. 6 clearly shows how the fracture runs along the individual fibres. The micrograph shows distinct regions separated from each other by fine cracks (Fig. 7). Along these cracks, which pass from the base of the deposit to its surface, FEMD can be cleft to individual needles. Many of these fine but broken needles can be found in the ground sample. Scanning electron micrographs demonstrate that the basic fibrous structure is even realized in very small dimensions and consists of leaf-like layers (Figs. 8b and c).

The fibrous structure of FEMD-S is less marked (Figs. 9a and b). It consists of columnar bundles, the front surface of these columns imparting to the whole of the surface the characteristic appearance of an irregular honeycomb structure (Fig. 9c). When FEMD-S is split, the individual fibres obtained have a less exact form than those of FEMD-N or FEMD-P, and the micrograph of FEMD-S presents etching patterns which point to

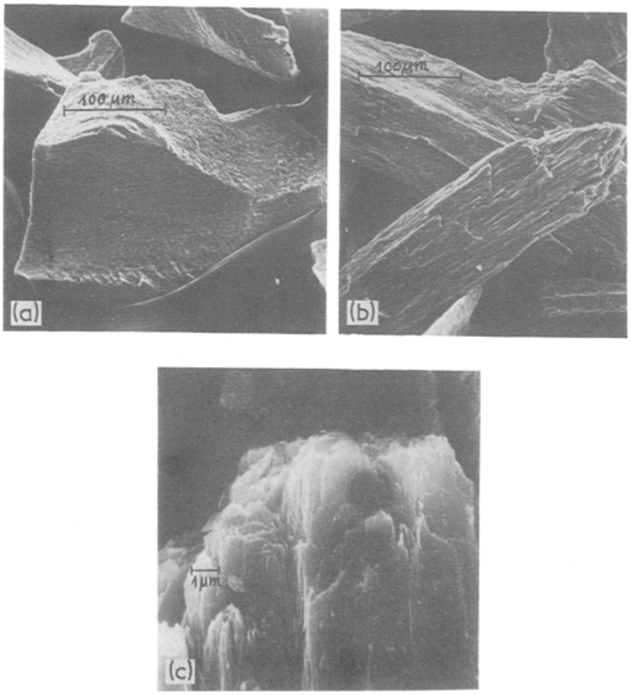

Fig. 8. Scanning electron micrographs of fractured surfaces. (a) EMD; (b) and (c) FEMD-N.

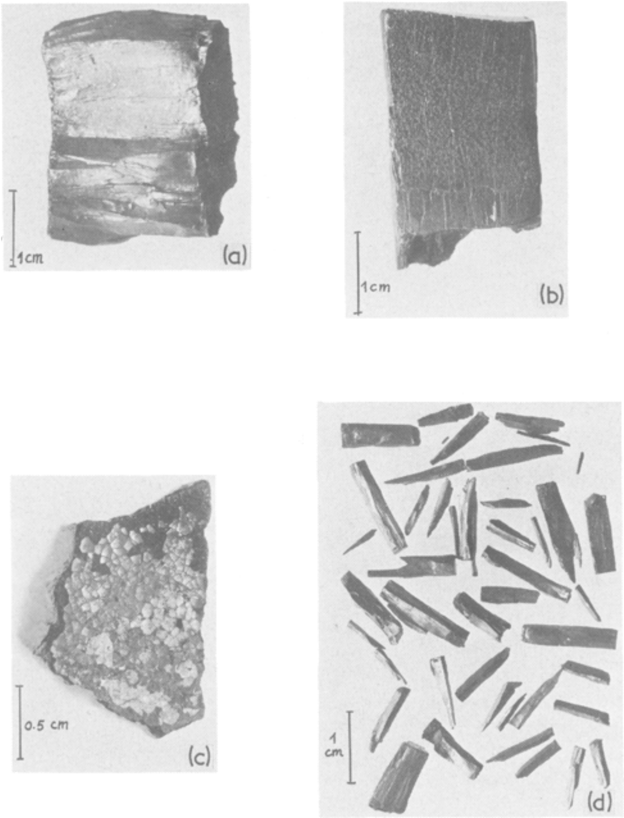

Fig. 9. FEMD-S. (a) Fragment; (b) surface of the as-grown sample; (c) section parallel to the direction of growth; (d) needle-like particles in the crushed material.

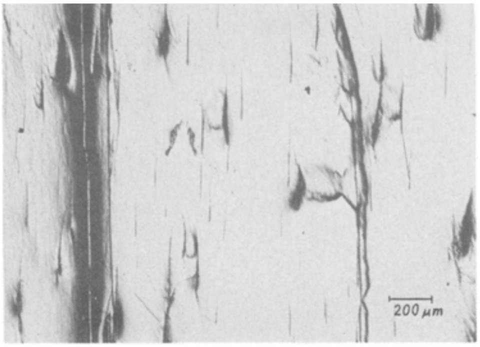

Fig. 10. FEMD-S. Section parallel to the direction of growth, polished and etched.

a strong and fairly regular disturbance of growth (Fig. 10). Crushed FEMD-S consists of many rodlets of different size in addition to irregular fragments (Fig. 9d).

7. Results obtained by X-ray diffraction

Whereas in the case of metal deposition the orientation of the crystal with respect to the direction of the applied electric field is the rule, a growth texture of electrolytic manganese dioxide was described for the first time by Koshiba and Nizhizawa [2] who showed that the intensities of the diffraction lines change with the change in the position of a block sample relative to the incident beam (Fig. 11, EMD). As compared with the intensity patterns for EMD the diagrams given by Amano *et al.* [3, 4] for FEMD-N and FEMD-C exhibit a significant difference regarding the line intensities (Fig. 11). Our findings revealed the well-known powder X-ray diagrams with all types of manganese dioxide under investigation. But when taking texture diagrams significant differences were observed between the group EMD,

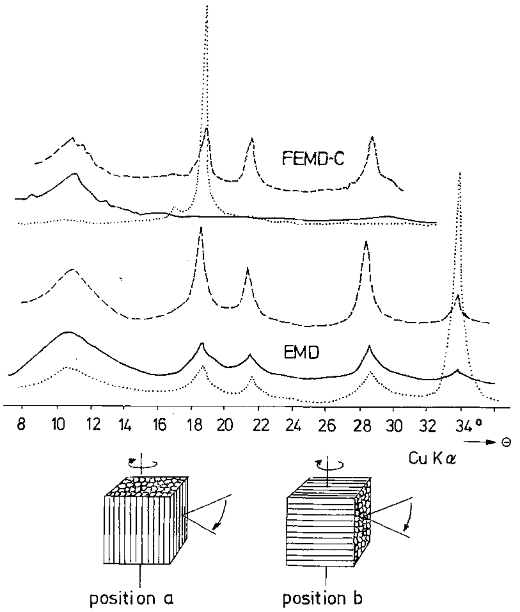

Fig. 11. Diffractometer tracings of FEMD-C and EMD according to the work of Amano *et al.* (FEMD-C) and Koshiba *et al.* (EMD). Position of the sample in the diffractometer: (solid line) according to (a); (dotted line) according to (b); (dashed line) powder sample. (The scale of calibration has been converted from FeKα to CuKα units of the diffraction angle as used in this paper).

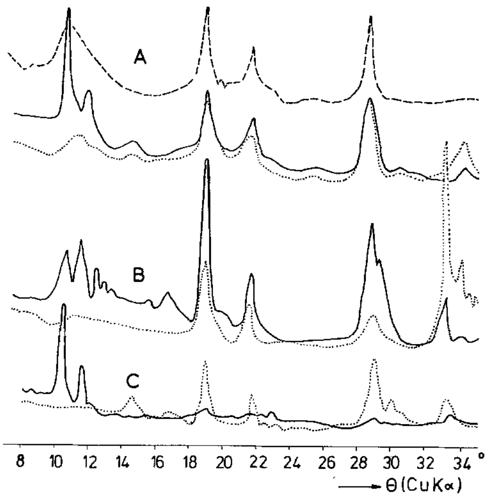

Fig. 12. Diffraction tracings obtained from solid blocks, type I. Position of the sample in the diffractometer: (solid line) according to (a) as indicated in Fig. 11; (dotted line) according to (b) as indicated in Fig. 11; (dashed line) powder sample. A: EMD-S; B: FEMD-S; C: HMD.

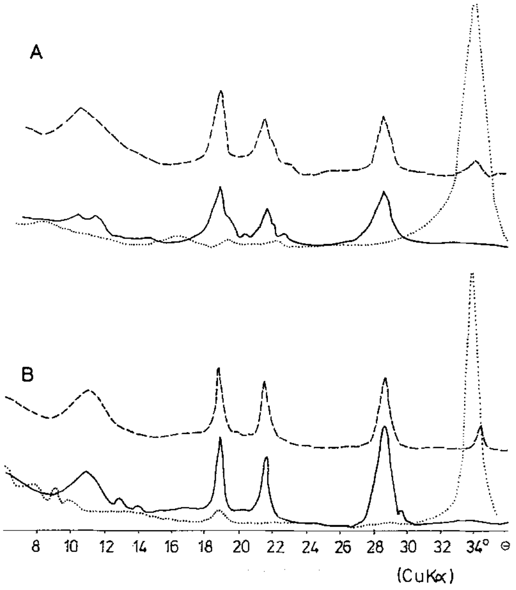

Fig. 13. Diffractometer tracings obtained from solid blocks, type II. Position of the sample in the diffractometer: (solid line) according to (a) as indicated in Fig. 11; (dotted line) according to (b); (dashed line) powder sample. A: FEMD-P; B: EMD-S, containing 0·1% vanadium.

FEMD-S and HMD and the group FEMD-N, FEMD-C and FEMD-P. The first group gives diffraction patterns in which the usually diffuse peak at $\theta = 11°$ (for CuKα radiation), corresponding to $d = 4{\cdot}04$ Å, is split into a group of at least two or perhaps three reflections, whereas the reflection at $\theta = 32{\cdot}5°$ ($d = 1{\cdot}43$ Å) is only slightly intensified (diagrams taken in position *a*, as indicated in Fig. 11). These diagrams are shown in Fig. 12 and are designated as type I.

The type II diagrams are found with FEMD-N, FEMD-C and FEMD-P as well as with the iron and vanadium-containing EMD samples and are shown in Fig. 13. They may be characterized by the fact that no significant deviation from the powder sample diagrams occur with diagrams taken in position *a*, but that only one strong reflection at $\theta = 34°$ ($d = 1{\cdot}38$) appears in diagrams taken in position *b*.

With regard to the intensity of the reflection at $\theta = 32{\cdot}5$, the diagram for FEMD-S resembles the diagram for EMD, given by Nishizawa and Koshiba. It is, however, surprising that the diagrams given by Amano *et al.* for their fibrous manganese dioxides are not identical with the diagrams of type II which we found with our preparations of fibrous manganese dioxide. It is true that the range of measurement which has been used by the

Japanese authors do not cover diffraction angles up to 33·5° at which FEMD-N and FEMD-P (as well as FEMD-C) in the case of position *b* have single peaks of very high intensity; but the only and very strong peak indicated with regard to this case is the peak at $\theta = 18{\cdot}5°$.

These essential differences suggest that during the growth of solid manganese dioxide the crystal lattice may be oriented in different positions with regard to the direction of growth and, in the case of fibrous manganese dioxide, with regard to the axis of the fibres.

From the splitting up of the reflection at $\theta = 11°$ into several individual reflections (Fig. 12) the conclusion may be drawn that EMD with X-ray diagrams of type I has an orientation which is such that in the case of the rotational axis being normal to the fibre axis Bragg's condition of interference is well-complied with for these lattice planes which can thus be recognized in spite of the considerably disturbed crystal structure. In type II, no splitting up of this reflection can be observed.

The experimental facts now available do not permit any conclusions to be drawn on the circumstances by which the orientations type I or II are caused to be formed. The rather obvious suggestion that type II is formed in sulphate baths has to be restricted by the observation that, in the presence of iron ions or quadrivalent vanadium, type II is formed also from the sulphate bath (Fig. 12).

The cleavage properties are also not coupled with the type of orientation, as neither vanadium-containing EMD nor EMD prepared from very pure hydrochloric acid-containing manganese chloride solutions are fibrous but both these kinds of manganese dioxide possess a texture of the type II.

To sum up it may be said that in most cases 'grown' γ-manganese dioxides have a growth texture and that really polycrystalline material which according to X-ray diffraction is isotropic is an exception.

In addition to what has been said it may be mentioned that α-manganese dioxide that has been deposited electrochemically [7] also has a growth texture, although this texture is but slightly marked.

8. Degree of crystallization of electrolytic manganese dioxide

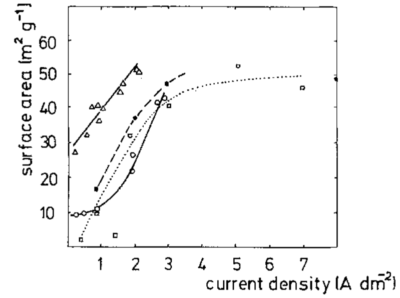

Fig. 14. BET surface area of electrodeposited manganese dioxide as a function of the anodic current density. □ FEMD-P; ○ FEMD-N; ● FEMD-C; △ EMD-S.

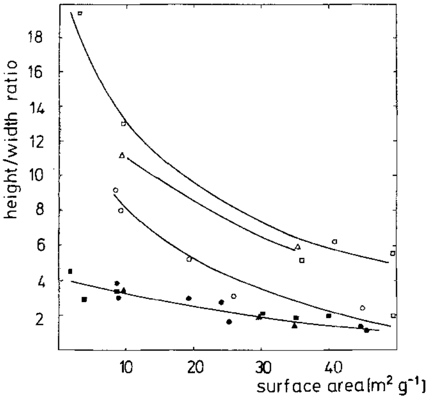

Fig. 15. Correlation between the sharpness of the reflections in the diffractometer tracings and the surface area of manganese dioxide samples. △ □ ○ reflections at $\theta = 18{\cdot}5°$; ▲ ■ ● reflections at $\theta = 28°$; □ ■ FEMD-P; ○ ● FEMD-N; △ ▲ EMD-S.

Whereas the density of electrolytic manganese dioxide and the degree of oxidation may be influenced by the conditions of electrolysis to a very insignificant degree only, there is a systematic relation between the BET surface and the anodic current density (Fig. 14). If the ratio of the height of the diffraction peaks to their width (determined on diagrams obtained by intensity measurements using a counting device) is taken as a measure by which the state of crystallization may be defined, it will be seen that the BET surface area is a function of the degree of crystallization, this interdependence being shown in Fig. 15. These relations can be explained by the assumption that, as the concentration of quadrivalent manganese ions increases, the manganese dioxide forming in the course of the secondary reaction is incorporated immediately in front of the surface of the dioxide at such a rate that the correct arrangement within the existing lattice becomes more and more difficult. The lattice of EMD is disturbed already when the anodic current density is very low while FEMD-P deposited at a current density of 0·25 A dm^{-2} has a BET surface area of not more than 3 $m^2 g^{-1}$ which is very low for electrodeposited manganese dioxide. Further work could check to what extent the efficiency of a certain type of manganese dioxide as a cathode in primary cells depends on parameters such as BET surface area and degree of crystallization.

Acknowledgment

The author wishes to thank the Head of Research of Hoechst AG, Bereich A, for permission to publish this paper and Dr J. A. Lee, London, for revision of the English manuscript.

References

[1] K. J. Takahashi, *Metals* 22 (1971) 64–67.
[2] J. Koshiba and S. Nishizawa, in 'Electrochemistry of Manganese Dioxide and Manganese Dioxide Batteries in Japan', U.S. Branch Office, The Electrochem. Soc. Japan, Cleveland, Ohio 1971, Vol. 2, pp. 85–99.
[3] Y. Amano, H. Kumano, A. Nishino and Y. Noguchi (to Matsushita Electric Ind. Co., Ltd), German Patent No. 1,796,305 (19 Dec. 1967).
[4] Matsushita Electric Ind. Co., Ltd, Japanese publ. specification No. 7,235,677 (11 Nov. 1968), published 7 Sept. 1972 (according to Derwent Patent Rep.).
[5] K. J. Vetter and G. Manecke, *Z. Phys. Chem.* 195 (1950) 337.
[6] A. Nishino, Lecture at the Meeting of The Electrochemical Society Boston, Mass. 7–11 Oct. 1973.
[7] E. Preisler, H. Harnisch and G. Mietens (to Knapsack Aktiengesellschaft), Deutsche Offenlegungschrift No. 2,026,597 (30 May 1970).